PHYSICAL REVIEW B **91**, 220503(R) (2015)

Interface-enhanced high-temperature superconductivity in single-unit-cell $FeTe_{1-x}Se_x$ films on $SrTiO_3$

Fangsen Li,[1] Hao Ding,[1] Chenjia Tang,[1] Junping Peng,[2] Qinghua Zhang,[2] Wenhao Zhang,[1] Guanyu Zhou,[1] Ding Zhang,[1] Can-Li Song,[1,3] Ke He,[1,3] Shuaihua Ji,[1,3] Xi Chen,[1,3] Lin Gu,[2,3] Lili Wang,[1,3,*] Xu-Cun Ma,[1,2,3] and Qi-Kun Xue[1,3,†]

[1]*State Key Laboratory of Low-Dimensional Quantum Physics, Department of Physics, Tsinghua University, Beijing 100084, China*

[2]*Institute of Physics, Chinese Academy of Science, Beijing 100190, China*

[3]*Collaborative Innovation Center of Quantum Matter, Beijing 100084, China*

(Received 12 April 2015; revised manuscript received 27 May 2015; published 17 June 2015)

Recently discovered high-temperature superconductivity in single-unit-cell (UC) FeSe films on $SrTiO_3$ (STO) substrate has stimulated tremendous research interest, both experimental and theoretical. Whether this scenario could be extended to other superconductors is vital in both identifying the enhanced superconductivity mechanism and further raising the critical transition temperature (T_c). Here we successfully prepared single-UC $FeTe_{1-x}Se_x$ ($0.1 \leqslant x \leqslant 0.6$) films on STO substrates by molecular beam epitaxy and observed U-shaped superconducting gaps (Δ) up to ~16.5 meV, nearly ten times the gap value ($\Delta \sim 1.7$ meV) of the optimally doped bulk $FeTe_{0.6}Se_{0.4}$ single crystal ($T_c \sim 14.5$ K). No superconducting gap has been observed on the second UC and thicker $FeTe_{1-x}Se_x$ films at 5.7 K, indicating the important role of the interface. This interface-enhanced high-temperature superconductivity is further confirmed by *ex situ* transport measurements, which revealed an onset superconducting transition temperature above 40 K, nearly two times higher than that of the optimally doped bulk $FeTe_{0.6}Se_{0.4}$ single crystal. This work demonstrates that interface engineering is a feasible way to discover alternative superconductors with higher T_c.

DOI: 10.1103/PhysRevB.91.220503 PACS number(s): 74.55.+v, 74.78.−w, 68.37.Ef

I. INTRODUCTION

Single-unit-cell (UC) FeSe films grown on $SrTiO_3$ (STO) substrate exhibit a superconducting gap up to 20 meV (Ref. [1]) and possible superconducting transition temperature above 100 K (Ref. [2]). The results are rather striking in terms of the fact that bulk FeSe only superconducts below 9 K (Ref. [3]) with $\Delta \sim 2.2$ meV (Ref. [4]). Despite intense experimental [5–12] and theoretical efforts [10,13–15], the mechanism for this giant enhancement is still elusive. What is significant is the important role of the STO substrates because neither the single-unit-cell (1UC) FeSe on graphene [4] nor the second-UC FeSe on STO (Ref. [1]) is superconducting. Interfacial charge transfer [5,6,9,12], strain [7,11], and enhanced electron-phonon coupling between FeSe and STO [1,10,14,15] have been suggested to account for the T_c enhancement.

Bulk FeTe, exhibiting similar crystal structure as FeSe, does not superconduct due to the developing of bicollinear antiferromagnetic ordering below 70 K. Se substitution to Te can suppress the magnetic order and induce superconductivity in FeTe, whose T_c increases with Se composition and reaches a maximum of 15 K at about 40% Se substitution [16]. In a previous low-temperature scanning tunneling microscopy (STM) and scanning tunneling spectroscopy (STS) study [17], it was found that the optimally doped bulk $FeTe_{0.6}Se_{0.4}$ exhibited a fully U-shaped superconducting gap $\Delta \sim 1.7$ meV with $T_c \sim 14.5$ K, which is higher than the maximum $T_c \sim 9$ K of bulk FeSe. Considering the fact of largely enhanced interface superconductivity in single-unit-cell (1UC) FeSe/STO, it is natural to ask whether a 1UC $FeTe_{1-x}Se_x$ film on STO is also superconducting and its T_c is higher. To test this idea, here we prepared 1UC $FeTe_{1-x}Se_x$ films ($0 \leqslant x \leqslant 0.6$) on STO(001) substrates by molecular beam epitaxy (MBE) and studied the superconducting properties by combined *in situ* STS study and *ex situ* transport measurement.

II. RESULTS AND DISCUSSIONS

High-quality 1UC $FeTe_{1-x}Se_x$ films with well-controlled stoichiometry were epitaxially grown on STO(001) substrates in UHV systems (see Supplemental Material [18]). Figures 1(a)–1(d) show typical atomic-resolution STM topographic images of 1UC $FeTe_{1-x}Se_x$ (nominal $x = 0$, 0.1, 0.3, 0.6) films, and reveal ordered Se- or Te-terminated (001) lattice. In Figs. 1(b)–1(d), bigger Te atoms are imaged brighter while smaller Se atoms are darker, which is consistent with previous observations in bulk $FeTe_{1-x}Se_x$ materials [19–21], and this contrast difference between Te and Se is independent of the sample bias applied. The methods to calculate the composition are described in the Supplemental Material [18]. Fourier analysis of our STM images reveals that the in-plane lattice constant varies little (within a range of $\sim 0.386 \pm 0.003$ nm) with Se/Te ratio (0.390 nm for $x = 0$, 0.384 nm for $x = 0.1$, 0.385 nm for $x = 0.3$, and 0.383 nm for $x = 0.6$), and is very close to the in-plane lattice constant ($a = 0.3905$ nm) of STO(001). The $FeTe_{1-x}Se_x$ film is thus tensile strained since its lattice constant is larger than that of bulk material ($a = 0.376$ nm for FeSe and $a = 0.382$ nm for FeTe). The out-of-plane roughness due to the contrast between Se and Te is up to 38 pm, close to the value due to the phase separation in bulk $FeTe_{1-x}Se_x$ ($0.6 \leqslant x \leqslant 0.8$) (Ref. [22]). This local separation between Se and Te clusters has been called nanoscale phase separation [21], in contrast to macroscopic phase separation in bulk $FeTe_{1-x}Se_x$.

*liliwang@mail.tsinghua.edu.cn
†qkxue@mail.tsinghua.edu.cn

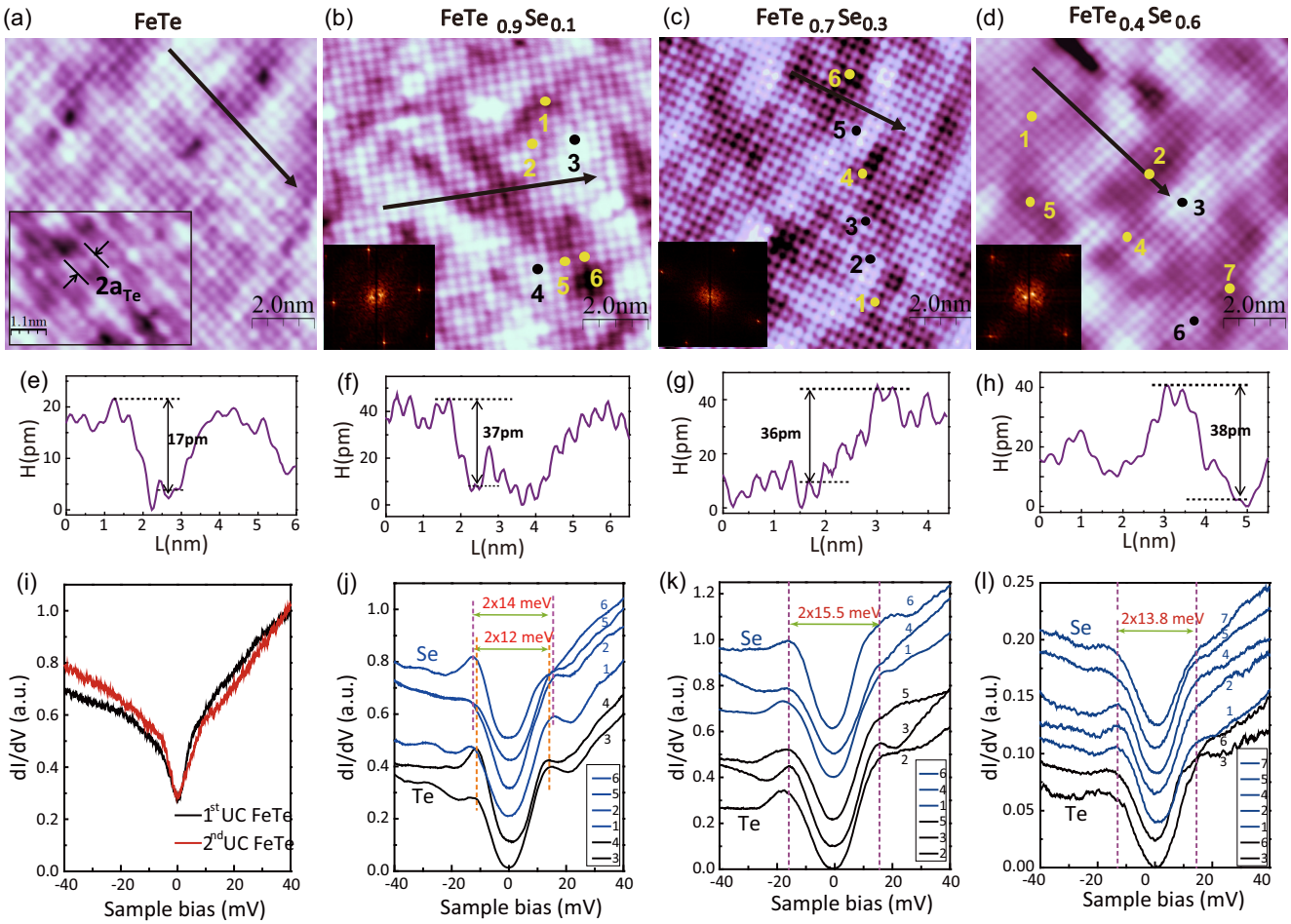

FIG. 1. (Color online) Atomically resolved STM images and dI/dV tunneling spectra of 1UC $FeTe_{1-x}Se_x$ films on STO(001). (a–d) STM topographies of 1UC $FeTe_{1-x}Se_x$ films, x = 0, 0.1, 0.3, and 0.6, respectively. The close-up image inserted in (a) ($V_b = 0.2$V, $I_t = 0.1$nA) shows charge-density wave (CDW)-like structure with period of $2a_{Te}$. The insets in (b–d) are the corresponding fast Fourier transformation images. (e–h) Surface corrugation along the black lines in (a–d), respectively. (i) Typical spectra taken on pure FeTe film on STO(001) at 0.4 K. (j–l) A series of dI/dV spectra taken on 1UC $FeTe_{1-x}Se_x$ films on STO ($x = 0.1$, 0.3, and 0.6) at 5.7 K, as marked in (b–d), respectively. Blue curves are taken on Se sites and black curves on Te sites.

We conducted tunneling spectroscopy experiments to investigate the superconducting property of the films. Figures 1(i)–1(l) show a series of dI/dV spectra on $FeTe_{1-x}Se_x$ surfaces with different stoichiometry ($x = 0, 0.1, 0.3, 0.6$). For pure FeTe films ($x = 0$), the dI/dV spectra of both the first UC and the second UC films show a dip yet finite density of states (DOS) at Femi energy, and no superconductinglike feature was observed down to 0.4 K [Fig. 1(i)], suggesting metallic behavior that is similar to that of the cleaved surface of bulk FeTe (Ref. [21]). The absence of superconductivity in FeTe films is probably due to the antiferromagnetic order as observed in bulk FeTe (Ref. [23]), for the charge density wave is observed here in 1UC FeTe on STO [see inset in Fig. 1(a)] and also in thicker FeTe films on graphene substrates [24]. On the other hand, Se-substituted 1UC FeTe films, 1UC $FeTe_{1-x}Se_x$, exhibit the signature of superconductivity: U-shaped superconducting gaps centered at Fermi level with one pair of two gap-edge coherence peaks are clearly revealed in Figs. 1(j)–1(l). Depending on the Se composition, the gap size varies from 12 to 16.5 meV. The value is at least six times larger than the SC gap $\sim$1.7 meV of the optimized doped bulk $FeTe_{0.6}Se_{0.4}$ single crystal (Ref. [17]). It is worthy to note that in contrast to the filamentary superconductivity reported in bulk $FeTe_{1-x}Se_x$ when the Se ratio is smaller than 0.29 (Ref. [25]), the SC gap is persistent on the whole surface of 1UC $FeTe_{1-x}Se_x$ films when the Se ratio is as low as 10%, even though the gap size seems somehow position dependent: $\Delta \sim 14 \pm 1.0$ meV on Se sites while $\Delta \sim 12 \pm 0.8$ meV on Te sites. The spatial inhomogeneity in gap size fades away with increasing Se concentration. As shown in Figs. 1(k) and 1(l), the 1UC $FeTe_{0.7}Se_{0.3}$ films and 1UC $FeTe_{0.4}Se_{0.6}$ films exhibit a spatially homogeneous gap, no matter where on the Te or Se sites the dI/dV spectra were acquired.

We plotted the normalized spectra of 1UC $FeTe_{1-x}Se_x$ films ($x = 0.1$, 0.3, 0.5, 0.6) in Fig. 2(a) (the method of spectrum normalization is specified in the Supplemental Material). Clearly, U-shaped gaps with vanishing conductance near the Fermi energy are observed. The statistics on SC gap size at each Se concentration are presented in Fig. 2(b), together with a phase diagram of bulk $FeTe_{1-x}Se_x$ for comparison [16,25,26]. The gap size is 13.8 ± 1.1 meV at $x = 0.1$,

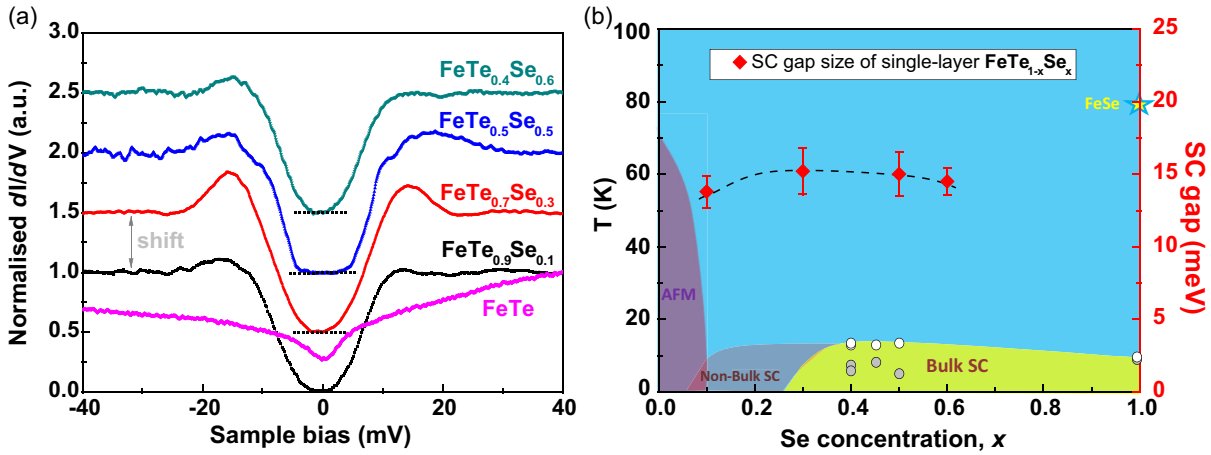

FIG. 2. (Color online) (a) Normalized dI/dV spectra of 1UC $FeTe_{1-x}Se_x$ films on STO(001). The spectra of $FeTe_{1-x}Se_x$, $x = 0.3$, 0.5, 0.6, are shifted by 0.5, relatively. The normalization process is specified in the Supplemental Material [18]. (b) Dependence of the SC gap on Se concentration x (red diamonds), together with the phase diagram of bulk materials [16,25,26]. The dashed line is a guide to eye. The SC gap (gray filled circle) (Refs. [17,20,21]) and onset temperature (white filled circle) (Refs. [16,25,26]) of bulk $FeTe_{1-x}Se_x$ are also labeled.

increases to 15.2 ± 1.6 meV at $x = 0.3$, reaches to a maximum of 15 ± 1.5 meV at $x = 0.5$, and decreases to 14.5 ± 1.0 meV at $x = 0.6$. The largest $\Delta \sim 16.5$ meV (see Fig. 5) is nearly ten times the $\Delta \sim 1.7$ meV (Ref. [17]) of the corresponding bulk $FeTe_{0.6}Se_{0.4}$ ($T_c \sim 14.5$ K). The enhancement of the gap, and thus the enhancement of the transition temperature, is expected.

To establish that the gap opening as observed in Fig. 1 corresponds to superconductivity transition in 1UC $FeTe_{1-x}Se_x$ films, we performed *ex situ* transport measurements using insulating STO substrates and a 10UC FeTe protection layer [8,9]. The normalized resistances $R/R_{300\,\mathrm{K}}$ and $R/R_{60\,\mathrm{K}}$ of the 10UC-FeTe/1UC-$FeTe_{0.5}Se_{0.5}$/STO sample as a function of temperature, T, are shown in Fig. 3. We can clearly observe that the resistance deviates from linear dependence at ~50 K and $R(T)/R_{60\,\mathrm{K}}$ drops completely to zero (within the instrumental resolution of ± 0.04 Ω) at 21 K. By extrapolating both the normal resistance and superconducting transition curves, we obtain the onset temperature of 40 K (see the lower inset in Fig. 3). The value is nearly three times the $T_c \sim 15$ K for bulk $FeTe_{0.5}Se_{0.5}$ (Ref. [16]). We further observe that the superconducting transition could be suppressed by external magnetic field (see the upper inset in Fig. 3), characteristic of superconductivity transition.

For comparison, we also plotted the normalized $R(T)/R_{300\,\mathrm{K}}$ and curves of 10UC-FeTe/1UC-FeSe/STO (Ref. [8]) in the main panel and the lower inset in Fig. 3, respectively. It is interesting to note that these two systems exhibit very similar R-T behavior and almost the same superconductivity transition. One of the possible explanations for the similarity is that substitution of Te for Se in 1UC $FeTe_{1-x}Se_x$ films takes place during growth of the 10UC FeTe protection layer under Te-rich condition. This is evidenced by surface corrugation change of 1UC FeSe films once the submonolayer FeTe is deposited, as shown in Fig. 4. Figure 4(a) displays an area where 1UC FeSe film coexists with 1UC FeTe islands on it. From Fig. 4(b), substitution of Te atoms (brighter dots) for Se (darker dots) is obvious, and the surface corrugation increases from 19 pm (black line profile) to about 38 pm (red line) after sub-UC FeTe is deposited. As a result, the superconducting gap of 1UC FeSe film decreases from 16.5 ± 1.0 meV to 10.5 ± 1.0 meV [Fig. 4(c)]. The pronounced double peak structure in Fig. 4(c) could point to multiple superconducting gaps. Considering the temperature dependence of the larger gap as revealed by previous ARPES [6] and STS study [1], we mainly compared the change of the larger gap. The substitution of Te for Se is further confirmed by a high-resolution scanning transmission

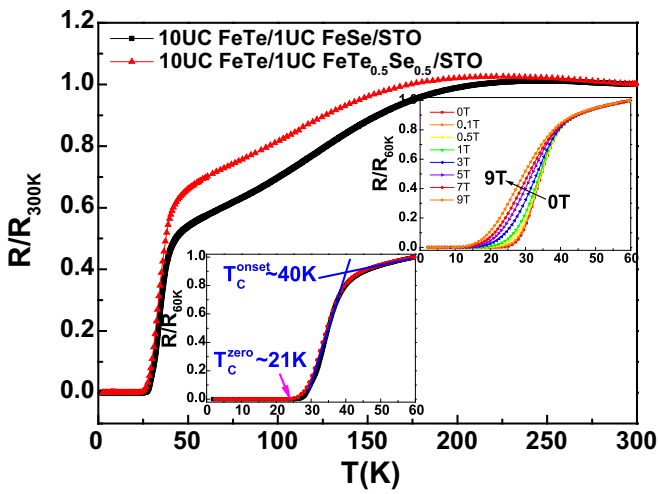

FIG. 3. (Color online) Transport property of 10UC − FeTe/1UC −$FeTe_{0.5}Se_{0.5}$/STO(001) heterostructure. Results of 1UC FeSe/STO (Ref. [8]) are also presented for comparison. Lower inset: normalized $R/R_{60\,\mathrm{K}}$-T curve of 10UC-FeTe/1UC-$FeTe_{0.5}Se_{0.5}$/STO(001) and 10UC-$rmFeTe/1UC$-FeSe/STO. Upper inset: $R/R_{60\,\mathrm{K}}$-T curves of 10UC-FeTe/1UC-$FeTe_{0.5}Se_{0.5}$/STO(001) under various magnetic fields applied along the direction perpendicular to the film.

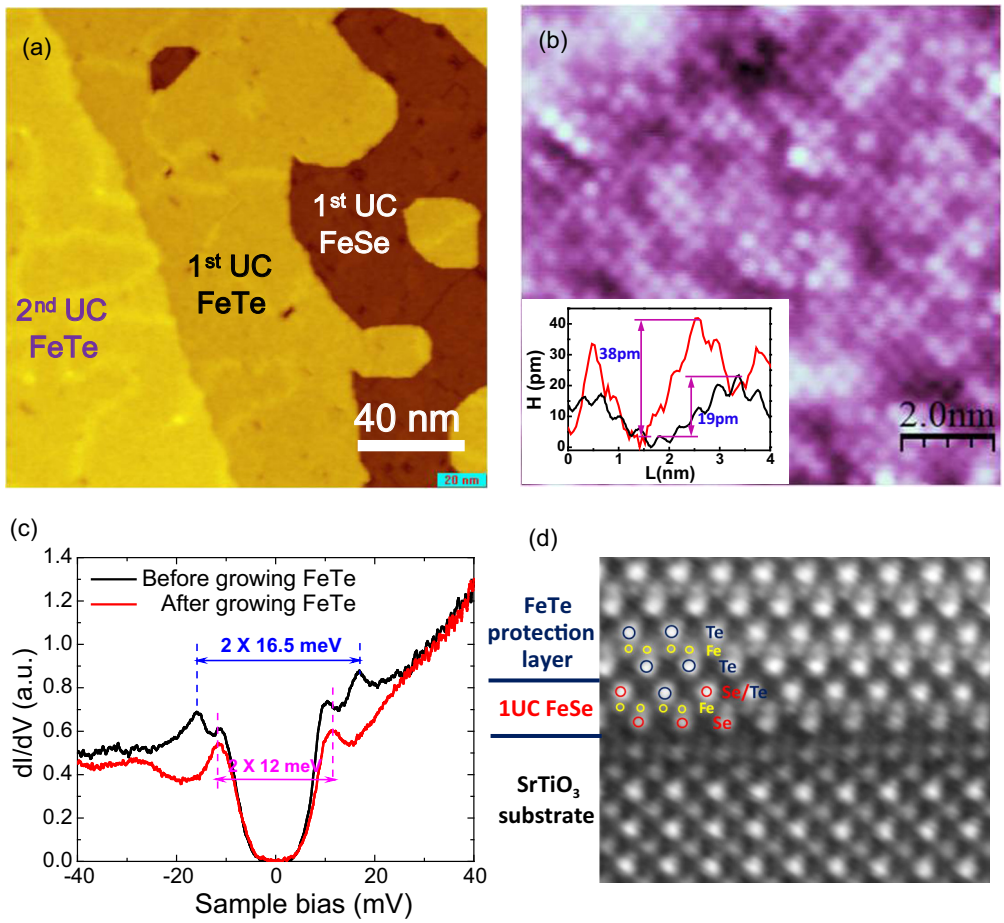

FIG. 4. (Color online) Effect of FeTe protection layer. (a) STM topography of the first UC FeSe film after the sub-UC FeTe film is deposited. (Adapted with permission from Ref. [8].) (b) Atomically resolved STM topographic images of exposed first UC FeSe area. Inset: Line profiles before and after sub-UC FeTe is deposited. (c) dI/dV spectra on first UC FeSe before and after sub-UC FeTe is deposited. (Adapted with permission from Ref. [8].) (d) STEM image of 10UC-FeTe/1UC-FeSe/STO heterostructure. The result that the top layer atoms in the Se-Fe-Se triple-layer structure are brighter than the bottom layer atoms reveals the mixture of Se/Te atoms, for the atomic number of Te is larger than Se atoms.

electron microscopy (STEM) image [Fig. 4(d)], as for the top layer Se atoms look similar to the Te layer in contrast and obviously brighter than the bottom layer Se atoms. The results imply that, due to interface intermixing of Se and Te, the transport data of 10UC-FeTe/1UC-FeSe/STO and 10UC-FeTe/1UC-$FeTe_{0.5}Se_{0.5}$/STO should both exhibit the property of 10UC-FeTe/1UC-$FeTe_{1-x}Se_x$/STO where the Se concentration x depends on the actual growth conditions used for preparing the multilayer films. The results may also explain why the T_c of 10UC-FeTe/1UC-FeSe/STO is lower than what is expected from the large gap (20 meV) observed on 1UC-FeSe/STO (Refs. [1,8]).

It is worthy to note that the second UC $FeTe_{1-x}Se_x$ film does not show superconductivity features down to 5.7 K. Shown in Fig. 5 are typical dI/dV spectra taken on the first UC (black curve) and the second UC (blue curve) $FeTe_{0.7}Se_{0.3}$ film. A metalliclike feature with finite density of states (DOS) near the Fermi energy is clearly revealed in the second UC film, while a well-defined superconducting gap of 16.5 meV shows up in the first UC film nearby. The result suggests the interface plays an important role in the enhanced superconductivity of single-UC $FeTe_{1-x}Se_x$ films on STO substrate. The important role of the interface is revealed by several differences between 1UC $FeTe_{1-x}Se_x$ films on STO and bulk $FeTe_{1-x}Se_x$. (1) 1UC $FeTe_{0.9}Se_{0.1}$ shows overall superconducting behavior rather than the filamentary superconductivity in the corresponding bulk material [25]. This can be partially attributed to the oxygen vacancies in STO substrate, for it was reported that O_2 annealing induces the evolution to bulk superconductivity for $FeTe_{1-x}Se_x$ ($x = 0.1$ and 0.4) [26], and coincidently, the STO substrate loses oxygen when it is heated during the sample growth and annealing. Moreover, interface charge transfer induced by oxygen vacancy in STO to FeSe films has been revealed as one of the main reasons for the interface-enhanced superconductivity [6,9]. (2) The bonding angle of Te-Fe-Te and the distance of Te or Se atoms away from the Fe plane have been reported to correlate with the T_c of ion-based superconductors [27]. In the case of 1UC $FeTe_{1-x}Se_x$ films on STO, the area of nanoscale phase separation and thus the bonding angle locally changes with different Se concentration x, which should lead to a change in the gap size and T_c. However, what we observed is different: the gap is nearly spatially homogeneous [see Figs. 1(k) and 1(l)] and gap size does not respond to such change over a wide composition range

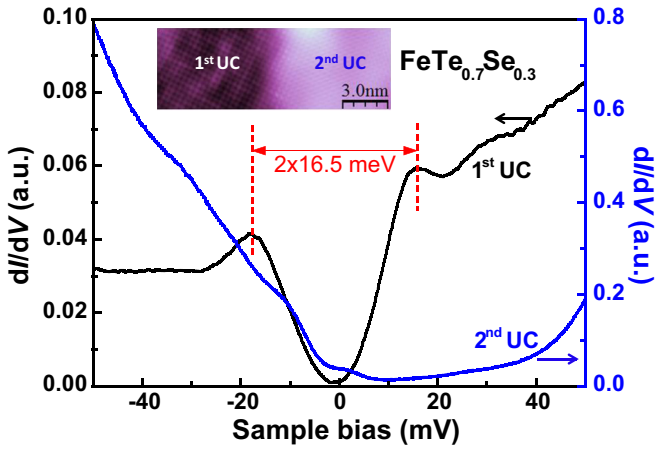

FIG. 5. (Color online) The dI/dV tunneling spectra of first UC and second UC $FeTe_{0.7}Se_{0.3}$ films on STO(001). Inset: STM topography (5 nm × 15 nm) of coexisting first UC and second UC $FeTe_{0.7}Se_{0.3}$ films.

($0.3 \leqslant x < 0.6$). All the above results demonstrate the deterministic role of the $FeTe_{1-x}Se_x$/STO interface in the enhanced superconductivity.

The large gap of 16.5 meV and the onset temperature of 40 K revealed by *ex situ* transport clearly indicate interface-enhanced high-temperature superconductivity in 1UC $FeTe_{1-x}Se_x$ film on STO. Then, it is critical to determine how high the T_c increases. In the case of 1UC FeSe films on STO, it has been reported that the electron coupling strength $2\Delta/k_BT_c$ is 6.8 ($\Delta \sim 19$ meV, $T_g \sim 65$ K, T_g is gap closing temperature) (Ref. [6]), well above the weak-coupling limit ~3.53 from Bardeen-Cooper-Schrieffer (BCS) theory, but close to the value (6.1) of bulk FeSe ($\Delta \sim 2.5$ meV, $T_c \sim 9.5$ K) (Refs. [28–30]). Assuming that the 1UC $FeTe_{1-x}Se_x$ films on STO hold similar pairing strength as that of bulk $FeTe_{1-x}Se_x$ ($\Delta \sim 1.7$ meV, $T_c \sim 14.5$ K, $2\Delta/k_BT_c \sim 2.72$) (Ref. [17]), the SC gap of ~16.5 meV implies a T_c much higher than the liquid nitrogen boiling point (77 K), which we leave for future experiments.

III. CONCLUSIONS

In conclusion, by combined *in situ* STM and STS and *ex situ* transport measurements, we have investigated the superconductivity of 1UC $FeTe_{1-x}Se_x$ films on STO. A significantly enhanced SC gap up to 16.5 meV is observed in a wide composition range ($0.1 \leqslant x \leqslant 0.6$), while the second UC and thicker $FeTe_{1-x}Se_x$ films do not exhibit any signature of superconductivity transition down to 5.7 K. While the pairing mechanism remains an interesting problem for further experimental and theoretical study, the work demonstrates an explicit and feasible way for rational design and preparation of high-T_c superconductors by interface engineering.

ACKNOWLEDGMENTS

The authors would like to thank Jiangping Hu and Shengbai Zhang for fruitful discussions. We are grateful to Ministry of Science and Technology of China and National Natural Science Foundation of China and Chinese Academy of Sciences for financial support.

[1] Q.-Y. Wang, Z. Li, W.-H. Zhang, Z.-C. Zhang, J.-S. Zhang, W. Li, H. Ding, Y.-B. Ou, P. Deng, K. Chang, J. Wen, C.-L. Song, K. He, J.-F. Jia, S.-H. Ji, Y.-Y. Wang, L.-L. Wang, X. Chen, X.-C. Ma, and Q.-K. Xue, Interface-induced high-temperature superconductivity in single unit-cell FeSe films on $SrTiO_3$, Chin. Phys. Lett. **29**, 037402 (2012).

[2] J.-F. Ge, Z.-L. Liu, C. H. Liu, C.-L. Gao, D. Qian, Q.-K. Xue, Y. Liu, and J.-F. Jia, Superconductivity above 100 K in single-layer FeSe films on doped $SrTiO_3$, Nat. Mater. **13**, 4153 (2014).

[3] F. C. Hsu, J. Y. Luo, K. W. The, T. K. Chen, T. W. Huang, P. M. Wu, Y. C. Lee, Y. L. Huang, Y. Y. Chu, D. C. Yan, and M. K. Wu, Superconductivity in the PbO-type structure α-FeSe, Proc. Natl. Acad. Sci. USA **105**, 14262 (2008).

[4] C.-L. Song, Y.-L. Wang, P. Cheng, Y.-P. Jiang, W. Li, T. Zhang, Z. Li, K. He, L. Wang, J.-F. Jia, H.-H. Hung, C. Wu, X. Ma, X. Chen, and Q.-K. Xue, Direct observation of nodes and twofold symmetry in FeSe superconductor, Science **332**, 1410 (2011).

[5] D. Liu, W. Zhang, D. Mou, J. He, Y.-B. Ou, Q.-Y. Wang, Z. Li, L. Wang, L. Zhao, S. He, Y. Peng, X. Liu, C. Chen, L. Yu, G. Liu, X. Dong, J. Zhang, C. Chen, Z. Xu, J. Hu *et al.*, Electronic origin of high-temperature superconductivity in single-layer FeSe superconductor, Nat. Commun. **3**, 931 (2012).

[6] S. L. He, J. F. He, W. H. Zhang, L. Zhao, D. F. Liu, X. Liu, D. X. Mou, Y. B. Ou, Q. Y. Wang, Z. Li, L. L. Wang, Y. Y. Peng, Y. Liu, C. Y. Chen, L. Yu, G. D. Liu, X. L. Dong, J. Zhang, C. T. Chen, Z. Y. Xu *et al.*, Phase diagram and electronic indication of high-temperature superconductivity at 65 K in single-layer FeSe films, Nat. Mater. **12**, 605 (2013).

[7] S. Tan, Y. Zhang, M. Xia, Z. R. Ye, F. Chen, X. Xie, R. Peng, D. F. Xu, Q. Fan, H. C. Xu, J. Jiang, T. Zhang, X. C. Lai, T. Xiang, J. P. Hu, B. P. Xie, and D. L. Feng, Interface-induced superconductivity and strain-dependent spin density wave in FeSe/$SrTiO_3$ thin films, Nat. Mater. **12**, 634 (2013).

[8] W. H. Zhang, Y. Sun, J. S. Zhang, F. S. Li, M. H. Guo, Y.-F. Zhao, H. M. Zhang, J. P. Peng, Y. Xing, H. C. Wang, T. Fujita, A. Hirata, Z. Li, H. Ding, C. J. Tang, M. Wang, Q. Y. Wang, K. He, S. H. Ji, X. Chen *et al.*, Direct observation of high temperature superconductivity in one-unit-cell FeSe films, Chin. Phys. Lett. **31**, 017401 (2014).

[9] W. H. Zhang, Z. Li, F. S. Li, H. M. Zhang, J. P. Peng, C. J. Tang, Q. Y. Wang, K. He, S. H. Ji, X. Chen, L. L. Wang, X. C. Ma, and Q.-K. Xue, Interfacial charge doping effect on superconductivity of single unit-cell FeSe films on $SrTiO_3$ substrates, Phys. Rev. B **89**, 060506(R) (2014).

[10] J. J. Lee, F. T. Schmitt, R. G. Moore, S. Johnston, Y.-T. Cui, W. Li, M. Yi, Z. K. Liu, M. Hashimoto, Y. Zhang, D. H. Lu, T. P. Devereaux, D.-H. Lee, and Z.-X. Shen, Interfacial mode coupling as the origin of the enhancement of Tc in FeSe films on $SrTiO_3$, Nature **515**, 245 (2014).

[11] R. Peng, H. C. Xu, S.Y. Tan, H. Y. Cao, M. Xia, X. P. Shen, Z. C. Huang, C. H. P. Wen, Q. Song, T. Zhang, B. P. Xie, X. G. Gong, and D. L. Feng, Tuning the band structure and superconductivity

in single-layer FeSe by interface engineering, Nat. Commun. **5**, 5044 (2014).

[12] J. F. He, X. Liu, W. H. Zhang, L. Zhao, D. F. Liu, S. L. He, D. X. Mou, F. S. Li, C. J. Tang, Z. Li, L. L. Wang, Y. Y. Peng, Y. Liu, C. Y. Chen, L. Yu, G. D. Liu, X. L. Dong, J. Zhang, C. T. Chen, Z. Y. Xu *et al.*, Electronic evidence of an insulator-superconductor crossover in single-layer FeSe/$SrTiO_3$ films, Proc. Natl. Acad. Sci. USA **111**, 18501 (2014).

[13] K. Liu, Z.-Y. Lu, and T. Xiang, Atomic and electronic structures of FeSe monolayer and bilayer thin films on $SrTiO_3$(001):First-principles study, Phys. Rev. B **85**, 235123 (2012).

[14] Y.-Y. Xiang, F. Wang, D. Wang, Q.-H. Wang, and D.-H. Lee, High-temperature superconductivity at the FeSe/$SrTiO_3$ interface, Phys. Rev. B **86**, 134508 (2012).

[15] S. Coh, M. L. Cohen, and S. G. Louie, Structural template increases electron-phonon interaction in an FeSe monolayer, arXiv:1407.5657.

[16] M.-K. Wu, M.-J. Wang, and K.-W. Yeh, Recent advances in β-$FeSe_{1-x}$ and related superconductors, Sci. Technol. Adv. Mater. **14**, 014402 (2013).

[17] T. Hanaguri, S. Niitaka, K. Kuroki, and H. Takagi, Unconventional s-wave superconductivity in Fe(Se,Te), Science **328**, 474 (2010).

[18] See Supplemental Material at http://link.aps.org/supplemental/10.1103/PhysRevB.91.220503 for details on MBE growth and the determinations of the chemical composition of $FeTe_{1-x}Se_x$ film on $SrTiO_3$(001) substrate.

[19] U. R. Singh, S. C. White, S. Schmaus, V. Tsurkan, A. Loidl, J. Deisenhofer, and P. Wahl, Spatial inhomogeneity of the superconducting gap and order parameter in $FeSe_{0.4}Te_{0.6}$, Phys. Rev. B **88**, 155124 (2013).

[20] W. Lin, Q. Li, B. C. Sales, S. Jesse, A. S. Sefat, S. V. Kalinin, and M. H. Pan, Direct probe of interplay between local structure and superconductivity in $FeTe_{0.55}Se_{0.45}$, ACS Nano **7**, 2634 (2013).

[21] X. B. He, G. R. Li, J. D. Zhang, A. B. Karki, R. Y. Jin, B. C. Sales, A. S. Sefat, M. A. McGuire, D. Mandrus, and E. W. Plummer, Nanoscale chemical phase separation in $FeTe_{0.55}Se_{0.45}$ as seen via scanning tunneling spectroscopy, Phys. Rev. B **83**, 220502(R) (2011).

[22] M. H. Fang, H. M. Pham, B. Qian, T. J. Liu, E. K. Vehstedt, Y. Liu, L. Spinu, and Z. Q. Mao, Superconductivity close to magnetic instability in $Fe(Se_{1-x}Te_x)_{0.82}$, Phys. Rev. B **78**, 224503 (2008).

[23] M. Enayat, Z. X. Sun, U. R. Singh, R. Aluru, S. Schmaus, A. Yaresko, Y. Liu, C. T. Lin, V. Tsurkan, A. Loidl, J. Deisenhofer, and P. Wahl, Real-space imaging of the atomic-scale magnetic structure of $Fe_{1+y}Te$, Science **345**, 653 (2014).

[24] W. Li, Wei-Guo Yin, L. L. Wang, K. He, X. C. Ma, Q.-K. Xue, and X. Chen, Charge-stripe order in a parent compound of iron-based superconductors, arXiv:1408.0057.

[25] T. J. Liu, J. Hu, B. Qian, D. Fobes, Z. Q. Mao, W. Bao, M. Reehuis, S. A. J. Kimber, K. Prokeš, S. Matas, D. N. Argyriou, A. Hiess, A. Rotaru, H. Pham, L. Spinu, Y. Qiu, V. Thampy, A. T. Savici, J. A. Rodriguez, and C. Broholm, From $(\pi, 0)$ magnetic order to superconductivity with (π, π) magnetic resonance in $Fe_{1.02}Te_{1-x}Se_x$, Nat. Mater. **9**, 718 (2010).

[26] Y. Kawasaki, K. Deguchi, S. Demura, T. Watanabe, H. Okazaki, T. Ozakim, T. Yamaguchi, H. Takeya, and Y. Takano, Phase diagram and oxygen annealing effect of $FeTe_{1-x}Se_x$ iron-based superconductor, Solid State Commun. **152**, 1135 (2012).

[27] Y. Mizuguchi and Y. Takano, Review of Fe chalcogenides as the simplest Fe-based superconductor, J. Phys. Soc. Japan **79**, 102001 (2010).

[28] S. Kasahara, T. Watashige, T. Hanaguri, Y. Kohsaka, T. Yamashita, Y. Shimoyama, Y. Mizukami, R. Endo, H. Ikeda, K. Aoyama, T. Terashima, S. Uji, T. Wolf, H. v. Löhneysen, T. Shibauchi, and Y. Matsuda, Field-induced superconducting phase of FeSe in the BCS-BEC cross-over, Proc. Natl. Acad. Sci. USA **111**, 16309 (2014).

[29] T. Kato, Y. Mizuguchi, H. Nakamura, T. Machida, H. Sakata, and Y. Takano, Local density of states and superconducting gap in the iron chalcogenide superconductor $Fe_{1+\delta}Se_{1-x}Te_x$ observed by scanning tunneling spectroscopy, Phys. Rev. B **80**, 180507(R) (2009).

[30] C. -L. Song, Y. Yin, M. Zech, T. Williams, M. M. Yee, G.-F. Chen, J.-L. Luo, N.-L. Wang, E. W. Hudson, and J. E. Hoffman, Dopant clustering, electronic inhomogeneity, and vortex pinning in iron-based superconductors, Phys. Rev. B **87**, 214519 (2013).